

RESEARCH ARTICLE

Open Access



The CB1 cannabinoid receptor regulates autophagy in the tibialis anterior skeletal muscle in mice

Carlos Sepúlveda^{1,2*}, Juan Manuel Rodríguez¹, Matías Monsalves-Álvarez³, Camila Donoso-Barraza¹, Francisco Pino-de la Fuente^{1,3}, Isabelle Matías⁵, Thierry Leste-Lasserre⁵, Philippe Zizzari⁵, Eugenia Morselli⁶, Daniela Cota⁵, Miguel Llanos^{1,7} and Rodrigo Troncoso^{1,4*} 

Abstract

The endocannabinoid system (ECS) regulates energy metabolism, has been implicated in the pathogenesis of metabolic diseases and exerts its actions mainly through the type 1 cannabinoid receptor (CB1). Likewise, autophagy is involved in several cellular processes. It is required for the normal development of muscle mass and metabolism, and its deregulation is associated with diseases. It is known that the CB1 regulates signaling pathways that control autophagy, however, it is currently unknown whether the ECS could regulate autophagy in the skeletal muscle of obese mice. This study aimed to investigate the role of the CB1 in regulating autophagy in skeletal muscle. We found concomitant deregulation in the ECS and autophagy markers in high-fat diet-induced obesity. In obese CB1-KO mice, the autophagy-associated protein LC3 II does not accumulate when mTOR and AMPK phosphorylation levels do not change. Acute inhibition of the CB1 with JD-5037 decreased LC3 II protein accumulation and autophagic flux. Our results suggest that the CB1 regulates autophagy in the tibialis anterior skeletal muscle in both lean and obese mice.

Keywords Endocannabinoid receptor, Skeletal muscle, Autophagy, High-fat diet

Background

Obesity has become a pandemic in modern societies, and its treatment is a complex public health concern, being the fifth leading cause of death worldwide [1]. Approximately ~28 million people around the world die as a result of overweight or obesity co-morbidities, including hypertension, dyslipidemia, insulin resistance, stroke, diabetes mellitus, fatty liver disease, coronary heart diseases, cancer, and metabolic diseases [2, 3]. Lifestyle modifications, nutritional, surgical, and pharmacological therapeutic strategies have been used to fight this condition [4]. Macroautophagy (herein referred to as autophagy) and the endocannabinoid system (ECS) are involved in the progress of obesity. Autophagy is a lysosome-dependent catabolic process whereby misfolded proteins and organelles are degraded and recycled for multiple processes [5]. The aberrant behavior of basal autophagy contributes to the

*Correspondence:

Carlos Sepúlveda
csepulvedag@ug.uchile.cl
Rodrigo Troncoso
rtroncoso@inta.uchile.cl

¹ Laboratorio de Investigación en Nutrición y Actividad Física (LABINAF), Instituto de Nutrición y Tecnología de los Alimentos (INTA), Universidad de Chile, Santiago, Chile

² Laboratorio de Ciencias del Ejercicio, Clínica MEDS, Santiago, Chile

³ Universidad de O'Higgins, Rancagua, Chile

⁴ Advanced Center for Chronic Diseases (ACCDiS), Universidad de Chile, 8380492 Santiago, Chile

⁵ University of Bordeaux, INSERM, Neurocentre Magendie, U1215, 33000 Bordeaux, France

⁶ Department of Basic Sciences, Faculty of Medicine and Sciences, Universidad San Sebastián, Santiago de Chile, Chile

⁷ Laboratorio de Hormonas y Regulación Metabólicas, Instituto de Nutrición y Tecnología de los Alimentos (INTA), Universidad de Chile, Santiago, Chile



© The Author(s) 2023. **Open Access** This article is licensed under a Creative Commons Attribution 4.0 International License, which permits use, sharing, adaptation, distribution and reproduction in any medium or format, as long as you give appropriate credit to the original author(s) and the source, provide a link to the Creative Commons licence, and indicate if changes were made. The images or other third party material in this article are included in the article's Creative Commons licence, unless indicated otherwise in a credit line to the material. If material is not included in the article's Creative Commons licence and your intended use is not permitted by statutory regulation or exceeds the permitted use, you will need to obtain permission directly from the copyright holder. To view a copy of this licence, visit <http://creativecommons.org/licenses/by/4.0/>. The Creative Commons Public Domain Dedication waiver (<http://creativecommons.org/publicdomain/zero/1.0/>) applies to the data made available in this article, unless otherwise stated in a credit line to the data.

pathogenesis of several diseases, including cancer, cardiovascular diseases, obesity, diabetes mellitus, and aging. In particular, disrupted autophagy in skeletal muscle is associated with lipid droplet accumulation, muscle mass imbalance, and metabolic homeostatic alterations [6–9]. For instance, intact autophagy is essential for preserving muscle structure and fitness under basal conditions [10]. Masiero et al. showed that autophagy-incompetent muscle progressively degenerates due to aberrant proteostasis [7]. Conversely, the stimulation of autophagy induces beneficial effects, such as retarding the age-dependent loss of muscle mass [11].

The ECS encompasses a large group of endogenous molecules, and the most studied endocannabinoids include arachidonylethanolamide (a.k.a. anandamide, AEA) and 2-arachidonoylglycerol (2-AG). Several enzymes are involved in their synthesis and degradation and two well-known G-protein coupled receptors, i.e., type 1 and type 2 cannabinoid receptors (CB1 and CB2) are involved in their signaling [12]. The main enzymes involved in the anandamide and 2-AG syntheses are the N-acyl phosphatidylethanolamine phospholipase D (Napepld) and diacylglycerol lipase alpha (Dagla), respectively. In addition, the identified hydrolyzing enzymes are fatty acid amide hydrolase (FAAH), which degrades anandamide, and monoacylglycerol lipase (MAGL), able to hydrolyze 2-AG. The CB1 is widely expressed in central and peripheral tissues, including the central nervous system, liver, adipose tissue, and skeletal muscle [13].

Diet-induced obesity leads to changes in the expression of the CB1, FAAH, and MAGL in several tissues and increased circulating endocannabinoids [14–16]. These changes affect the architecture and physiology of skeletal muscle, as previously described [17, 18]. From a general perspective, the ECS affects food intake and energy metabolism; for instance, pharmacological inhibition of CB1 by SR141716 (Rimonabant) reversed the obesity complications in rodents and improved several metabolic processes [19, 20]. Moreover, the CB1 is required for the development of diet-induced steatosis, dyslipidemia, and insulin and leptin resistance [21]. Treatment with a CB1 agonist increases *de novo* fatty acid synthesis in the liver or isolated hepatocytes, thus contributing to diet-induced obesity [15] and strongly suggesting a role in the progress of obesity and its comorbidities.

On the other hand, CB1 is known to influence mTOR and AMPK signaling (both known signaling pathways that regulate autophagy) [22, 23]. Although it is known that the CB1 participates in autophagy regulation in neurons [24, 25], it is unclear if the CB1 can modulate autophagy by canonical pathways *in vivo* in the tibialis anterior muscle. Furthermore, many studies have investigated the role of the ECS in regulating energy balance and metabolism

in the nervous system and peripheral organs [14, 16, 26], however, very few have examined the physiological role in skeletal muscle and, specially, the control of relevant biological processes, such as autophagy. This study aims to investigate the role of the CB1 in regulating autophagy in the tibialis anterior muscle. Here, we show evidence that the CB1 regulates basal autophagy in the tibialis anterior muscle in normal and diet-induced obese mice.

Results

A high-fat diet affects the ECS and autophagy in the tibialis anterior muscle

As previously suggested, exposure to a high-fat diet (HFD) leads to the deregulation of several biological systems [27–29]. We focused on the tibialis anterior (TA) skeletal muscle due to previous reports showing that autophagy modulation in this muscle is key to maintaining muscle mass [7, 30, 31]. As we expected, body weight, fasting glycemia, and area under the curve (AUC) of an intraperitoneal glucose tolerance test were increased in mice fed with a HFD for 12 weeks (Fig. 1A–E; * $p < 0.05$; ** $p < 0.01$; *** $p < 0.001$; and **** $p < 0.0001$). We found an increase in CB1 mRNA and protein levels in the TA in the HFD group (Fig. 1E–I; * $p < 0.05$). Moreover, mRNA expression was reduced for FAAH and increased for MAGL (Mgll), respectively, in the TA of mice fed with a HFD (Fig. 1F, G; * $p < 0.05$). To evaluate the effect of diet-induced obesity on autophagy markers, we then measured the protein levels of LC3 and p62/Sqstm1 (markers) in TA muscle. No significant changes were observed in the p62/Sqstm1 ratio. However, LC3 I and LC3 II accumulation was observed in the HFD group (Fig. 1J–M; ** $p < 0.01$ and *** $p < 0.001$). These results suggest that diet-induced obesity increases ECS activity and LC3 II protein levels.

Deletion of the CB1 prevents LC3 II accumulation induced by a high-fat diet in the tibialis anterior muscle

Since we observed concomitant deregulation in the ECS and basal autophagy markers, we wanted to determine if the deletion of the CB1 prevented LC3 II accumulation induced by a HFD in the TA. We fed CB1-KO male mice with a control or a HFD for 12 weeks (Fig. 2A). Genetic deletion of CB1 was confirmed by western blot analysis of TA (Supp. 1A). As previously reported [32], we found that CB1-KO mice were protected from diet-induced obesity, compared to WT controls, in terms of body weight, fat mass, and tibialis anterior weight, with no changes in lean mass (Fig. 2B–F). There was a lower cumulative calorie intake effect in mice with deletion of CB1 (Fig. 2G). HFD increased plasma glucose levels, but CB1 deletion prevented this hyperglycemia (Fig. 2H). Next, we evaluated endocannabinoids plasma concentrations. Mice fed

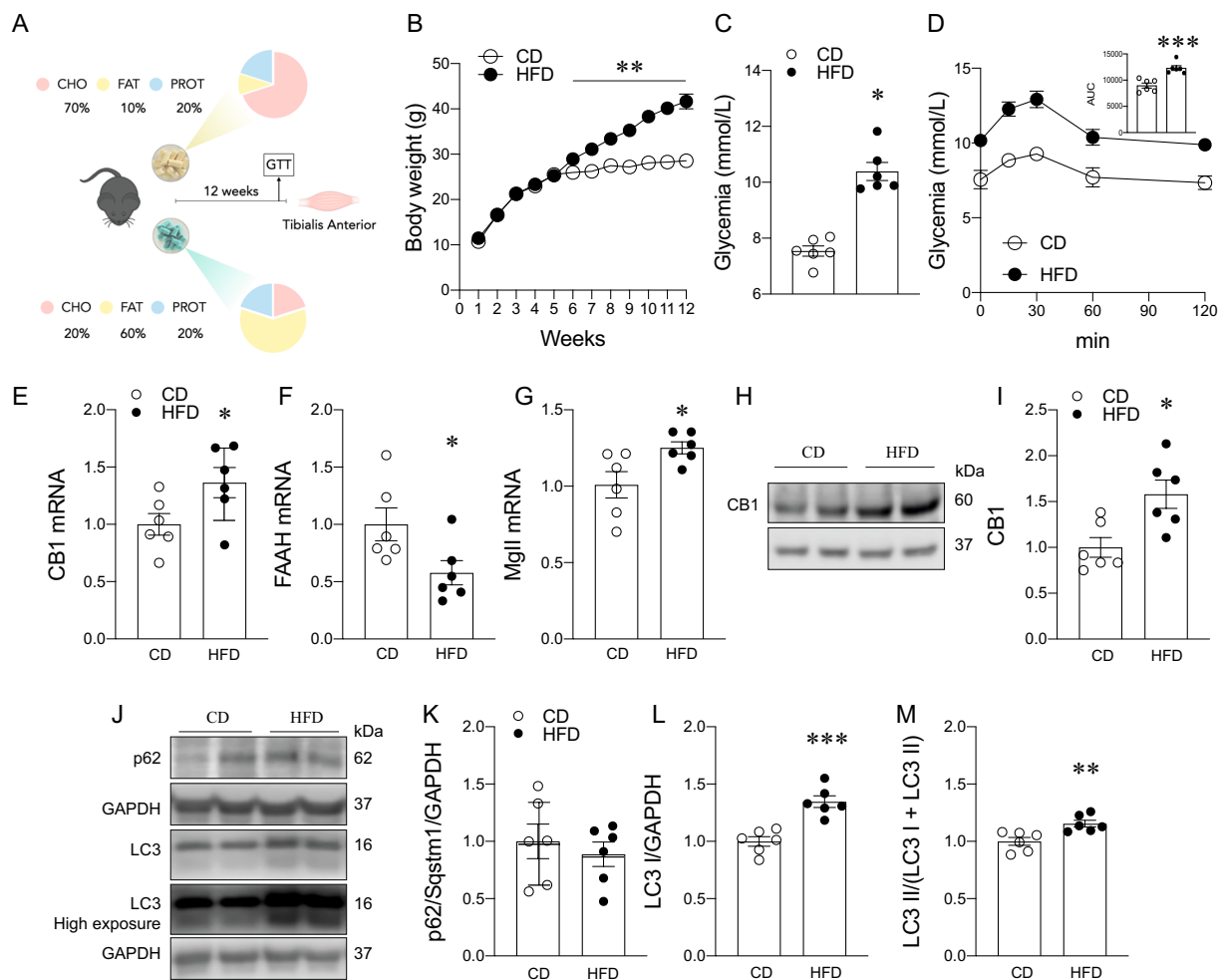


Fig. 1 Effects of a high-fat diet on body weight, glucose homeostasis, endocannabinoid system, and autophagy markers. **A** Study design. **B** Body weight. **C** Glycemia. **D** Glucose tolerance test (GTT). **E** Expression of CB1 mRNA levels. **F** Expression of FAAH mRNA levels (fatty acid amide hydroxylase). **G** Expression of monoacylglycerol lipase (MglI) mRNA levels. **H-I** CB1 protein levels. **J** Representative western blot. **K** p62/Sqstm1 protein levels. **L** LC3 I protein levels. **M** LC3 II normalized by total LC3. Two-way analysis of variance (ANOVA) repeated measurements with Bonferroni's post hoc test and unpaired t-test were conducted. * $p < 0.05$; ** $p < 0.01$; *** $p < 0.0005$; **** $p < 0.0001$. Values are expressed as mean and S.E.M. and scatter dot plots, as appropriate

with a HFD increased AEA and PEA plasma levels (Diet: $p < 0.0001$). Moreover, OEA levels increased by genotype and diet effect (Diet: $p = 0.0088$; Genotype: $p = 0.0243$) (Fig. 2I–L). We then explored the effect of diet-induced obesity on the mRNA expression of genes of the endocannabinoid system and autophagy in the TA. As shown in Fig. 3M, MglI and Napepld revealed a diet effect ($p < 0.05$), suggesting an increase of both enzymes. An interaction effect ($p < 0.05$) was found in Dag1 β , showing restoration of mRNA levels in HFD-fed CB1-KO mice. Finally, Becn1 had a diet and interaction effect ($p < 0.05$), indicating that a HFD increases its mRNA expression levels, and that the genotype further increases it.

To investigate whether CB1 knockout prevented LC3 II accumulation induced by a high-fat diet, we determined autophagy-related proteins levels. No significant changes were observed in p62/Sqstm1 and LC3 I protein levels (Fig. 3A–C). Interestingly, a diet and genotype effect ($p < 0.0001$) was found in LC3 II (Fig. 3D), suggesting a role for the CB, independently of the diet. To further elucidate if the genotype effect of LC3 II accumulation was driven by changes in the regulator proteins of autophagy, we evaluated the levels of AMPK and AKT/mTOR/p70S6K phosphorylation, which, unexpectedly, did not change (Fig. 3E–I).

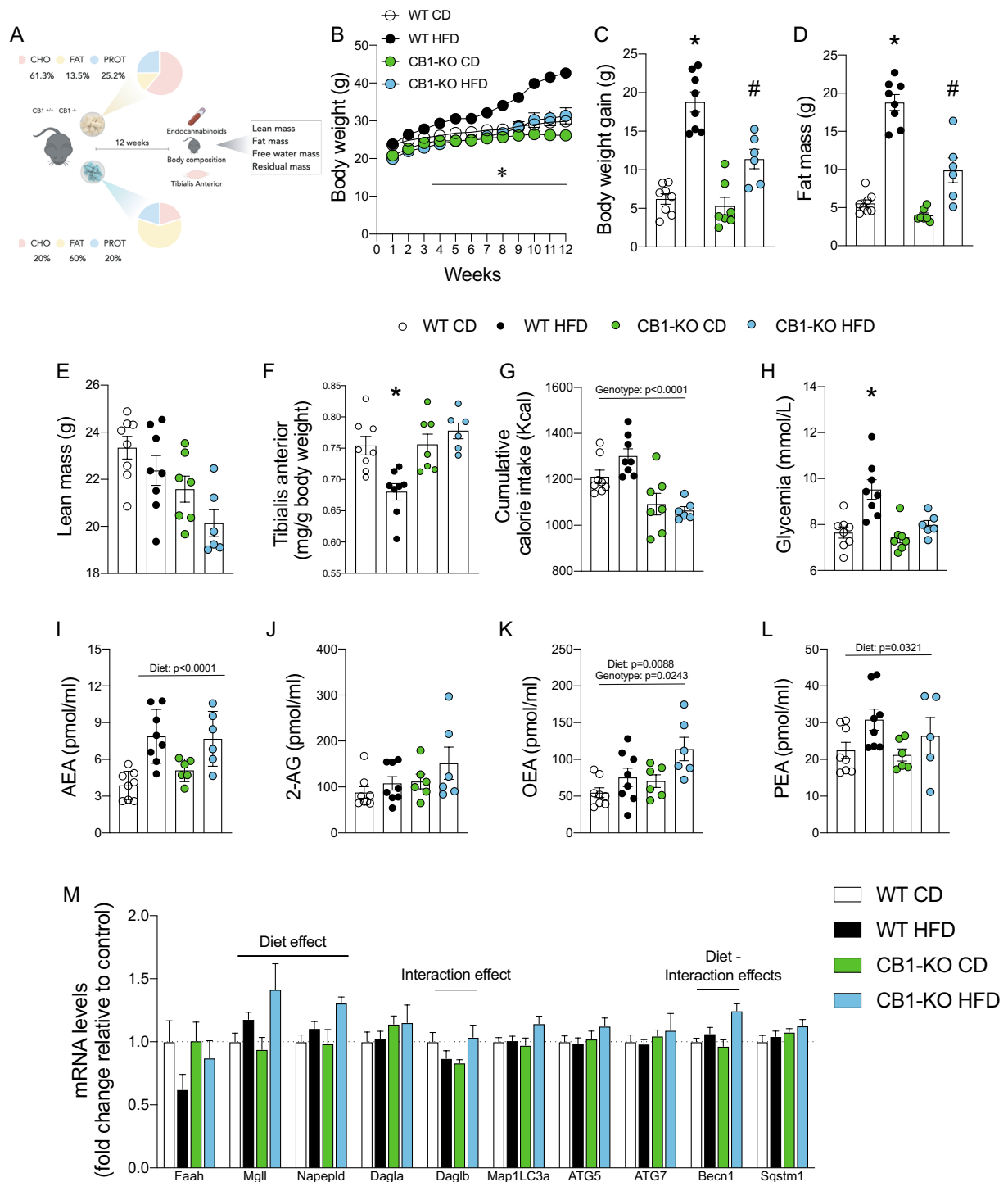


Fig. 2 Knockout of CB1 prevents impairment induced by a high-fat diet. **A** Study design. **B** Body weight gain curve. **D** Fat mass. **E** Lean mass. **F** Tibialis anterior weight. **G** Cumulative calorie intake. **H** Glycemia. **I** Plasma anandamide (AEA). **J** 2-arachidonoylglycerol (2-AG). **K** N-palmitoyl-ethanolamine (PEA). **L** Oleoylethanolamine (OEA). **M** mRNA levels. Two-way analysis of variance (ANOVA) repeated measurements with Bonferroni's post hoc test. Statistical significance was set at $p < 0.05$. *WT HFD vs. all groups. # CB1-KO HFD vs. WT CD and CB1-KO CD. Statistical significance was set at $p < 0.05$. Values are expressed as mean and S.E.M. and scatter dot plot, as appropriate

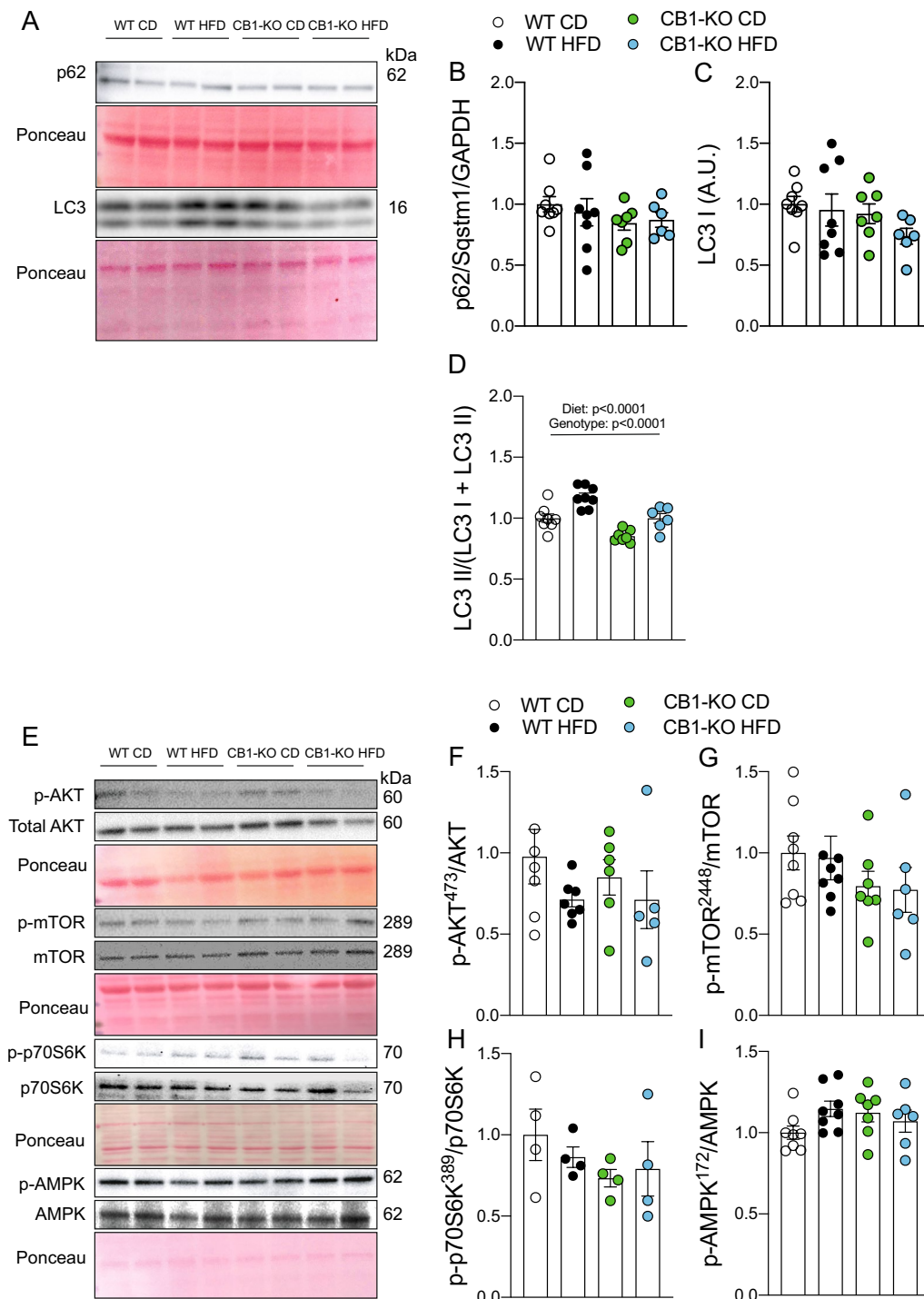


Fig. 3 Knockout CB1 prevents LC3 II accumulation in tibialis anterior muscle. p62/Sqstm1, LC3, AKT⁴⁷³, total AKT, mTOR²⁴⁴⁸, total mTOR, p70S6K³⁸⁹, total p70S6K, AMPK¹⁷², and total AMPK protein levels were determined by western blot. **A** Representative western blot image. **B** p62/Sqstm1 protein levels. **C** LC3 I protein levels. **D** LC3 II normalized by total LC3. **E** Representative western blot image. **F** AKT⁴⁷³. **G** mTOR²⁴⁴⁸. **H** p70S6K³⁸⁹. **I** AMPK¹⁷². Two-way analysis of variance (ANOVA) with Bonferroni's post hoc test. Statistical significance was set at $p < 0.05$. Values are expressed as mean and S.E.M. and scatter dot plots, as appropriate

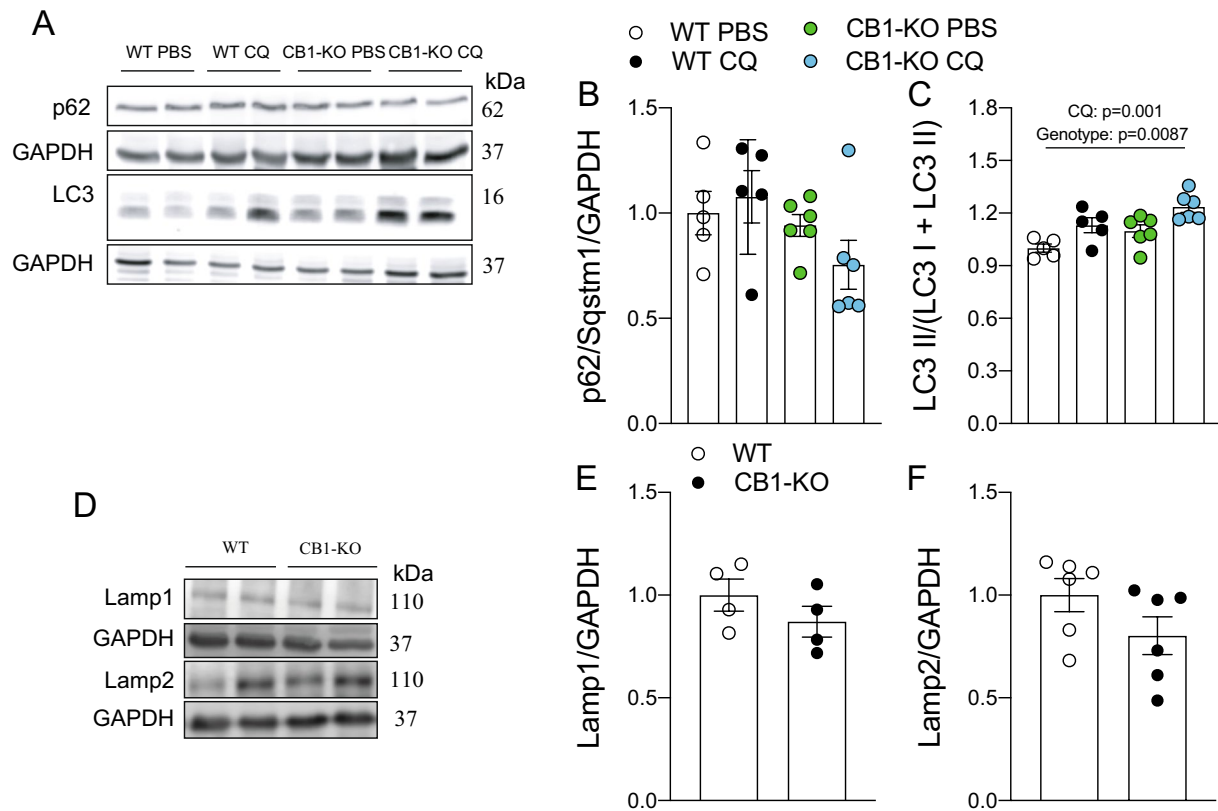


Fig. 4 The CB1 regulates basal autophagy in tibialis anterior muscle. p62/Sqstm1, LC3, Lamp1, and Lamp2 protein levels were determined by western blot. **A** Representative western blot image. **B** p62/Sqstm1 protein levels. **C** LC3 II is normalized by total LC3. **D** Representative western blot image. **E** Lamp1 protein levels. **F** Lamp2 protein levels. Two-way analysis of variance (ANOVA) with Bonferroni's post hoc test and unpaired *t*-test were conducted. Statistical significance was set at $p < 0.05$. Values are expressed as mean and S.E.M. and scatter dot plots, as appropriate

The CB1 regulates basal autophagy

Due to the surprising absence of changes in the protein phosphorylation of AMPK and the mTOR pathway, we evaluated whether the CB1 regulated autophagic flux by using chloroquine in WT and CB1-KO mice. We found no difference in p62/Sqstm1 protein levels (Fig. 4A, B). As we expected, chloroquine induced LC3 II accumulation (CQ: $p=0.001$ and Genotype: $p=0.0087$, Fig. 4C). To explore whether changes in the LC3 proteins in the second experiment with the HFD were the results of alterations in the lysosome, we then evaluated the Lysosomal-associated proteins 1 (Lamp1) and 2 (Lamp2), but there were no changes (Fig. 4D–F). To determine if pharmacological inhibition of the CB1 increased autophagic flux, we injected C57 mice intraperitoneally with a dose of JD-5037 (3 mg kg^{-1} body weight), which is a CB1 antagonist with low brain penetration [33]. An interaction effect was found in the JD+CQ group in p62/Sqstm1 protein levels (Interaction: $p=0.0085$; Fig. 5A, B). Regarding LC3 proteins, JD-5037 produced an effect ($p=0.0002$), suggesting that pharmacological blockade of CB1 prevents chloroquine-induced changes

in autophagic flux. Lastly, we observed an accumulation of polyubiquitinated protein in mice injected with JD-5037 (JD-5037 effect: $p=0.0163$). These results suggest that while genetic deletion of CB1 does not regulate autophagic flux, acute pharmacological inhibition of the CB1 with JD-5037 decreases LC3 II protein accumulation and autophagic flux.

Discussion

In this study, we investigated the role of CB1 in regulating autophagy in the TA skeletal muscle. We found an association between ECS deregulation and impaired basal autophagy in mice fed with a HFD. The alterations of the ECS were mainly characterized by a rise in the CB1 and a reduction of FAAH. On the other hand, interestingly, these results may constitute a concerted mechanism to activate CB1 with anandamide, its natural agonist. In addition, LC3 II accumulation is the distinctive point of autophagy impairment. We observed that the deletion of the CB1 in mice fed with a HFD prevented LC3 II accumulation, supporting the role of CB1 in favoring the increase of LC3 II observed in HFD. However, there was

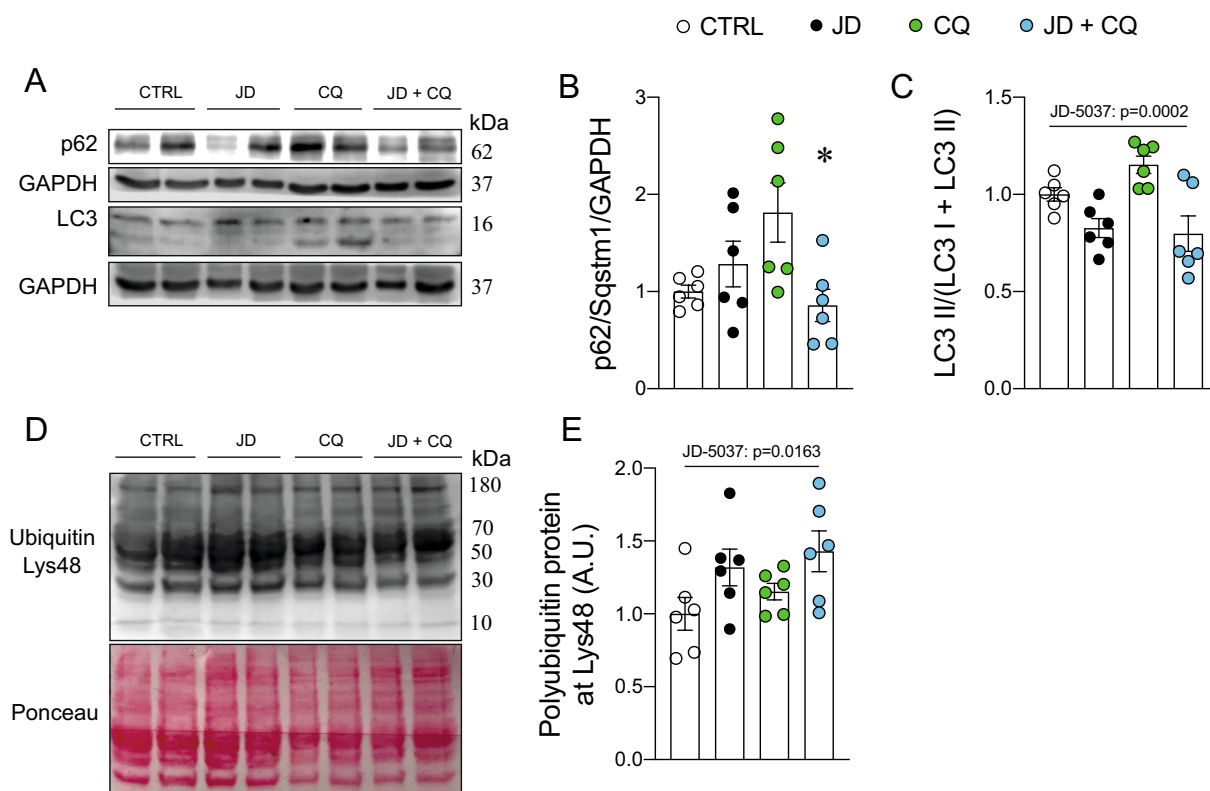


Fig. 5 JD-5037 reduces LC3 II protein in vivo. p62/Sqstm1, LC3, and polyubiquitin protein levels were determined by western blot. **A** Representative western blot image. **B** p62/Sqstm1 protein levels. **C** LC3 II is normalized by total LC3. **D** Representative western blot image. **E** Polyubiquitin protein levels. A two-way analysis of variance (ANOVA) with Bonferroni's post hoc test was conducted. Statistical significance was $p < 0.05$. *CQ vs. JD + CQ. Values are expressed as mean and S.E.M. and scatter dot plot, as appropriate

no change in the phosphorylation levels of the AMPK and mTOR pathways, two critical regulatory pathways of autophagy. Finally, while genetic deletion of CB1 regulated autophagy, acute pharmacological inhibition of the CB1 with JD-5037 decreased LC3 II protein accumulation and autophagic flux.

Previous studies have found an increase in CB1 levels in the liver, adipose tissue, and central nervous system of mice and humans with obesity [15, 34–37]. Accordingly, we found that CB1 mRNA and protein levels were increased in the TA of mice fed with a HFD. This fact could be relevant to muscle metabolism and physiology. Esposito et al. [18] exposed differentiated L6 skeletal muscle cells to SR141716 (Rimonabant), a known CB1 antagonist/inverse agonist, increasing 2-deoxyglucose uptake in a time- and dose-dependent manner. A similar effect was also induced by gene silencing of the CB1. In accordance, Liu et al. [38] treated female mice with a daily i.p. dose of Rimonabant, increasing glucose uptake by 68% in an isolated soleus muscle preparation. In addition, oxygen consumption was higher in Rimonabant- compared with vehicle-treated muscle. These reports corroborate the significant role of CB1 in muscle metabolism

and physiology. Additionally, we found decrease FAAH mRNA expression, suggesting reduced activity and, as a result, a possible rise of anandamide at the plasmatic and tissue levels, which may lead to persistent receptor activation [39]. Sipe et al. [40] studied a missense polymorphism in FAAH in 2667 subjects of white, black, and Asian ancestry. Their results indicate that FAAH polymorphism is a risk factor in the overweight/obese population. A role for this enzyme in energy homeostasis has also been shown in FAAH-deficient (FAAH^{-/-}) mice. These FAAH^{-/-} animals had increased total adipose tissue and body weight, and increased levels of anandamide in several tissues [41].

Aberrant autophagy has been reported in several tissues in obese mice [6, 42, 43]. Our findings show that basal autophagy is affected by diet-induced obesity in the tibialis anterior. Furthermore, decreased muscle mass has been found in mice fed with a HFD [44], and CB1-KO mice were protected from this effect. LC3 II accumulation correlates with either enhanced autophagosome synthesis or reduced autophagosome turnover, probably due to delayed trafficking to the lysosome, reduced fusion between compartments, or impaired lysosomal

proteolytic activity [45]. Fan and Xiao [46] showed that autophagy was compromised in the muscle of rats fed with a HFD. The authors fed rats with an HFD and then treated them with the autophagy inhibitor chloroquine. Using immunostaining and western blot, they found that the LC3 II/I ratio was increased in the muscle of rats fed with a HFD, denoting impaired autophagy. In agreement, Li et al. [47] showed that a HFD inhibits the production of autophagic lysosomal expression of autophagy-related genes (LC3 II, Becn1, and ATG5) and increases the accumulation of p62/Sqstm1 in the gastrocnemius muscle. Our findings show that basal autophagy is affected by diet-induced obesity. Therefore, our results suggest concomitant impairments in the ECS and autophagy in the TA.

Autophagy is a conserved cellular degradation process in which parts of the cytosol and organelles are sequestered into an autophagosome and delivered into a lysosome for breakdown and eventual recycling of the resulting macromolecules. Genetic deletion of the CB1 prevented the LC3 II accumulation induced by a HFD. We can speculate that decreased LC3 II levels reflect the restoration of autophagy, an explanation that requires further study. Unexpectedly, mTOR and AMPK, the two multiprotein complexes involved in the canonical induction pathway of autophagic vesicle formation, do not seem to be altered in our experimental setting. Autophagy is also regulated by non-canonical pathways that lead to autophagosomal degradation [48]. These alternative pathways are stimuli and cell-type dependent, thus future studies are required to better understand the mechanism that leads to this non-canonical autophagy regulation.

Autophagic flux assay is considered the best characterization of autophagy levels [49, 50]. Hence, we performed an autophagic flux assay *in vivo* in CB1-KO mice treated with an *i.p.* injection of chloroquine. We found higher LC3 II accumulation in wild-type and CB1-KO mice previously treated with chloroquine and, unexpectedly, lack of the CB1 did not affect LC3 II abundance. However, mice treated only with a CB1 antagonist, JD-5037, reduced LC3 II basal levels. Furthermore, JD-5037 reverted LC3 II accumulation by blocking chloroquine-induced fusion of the autophagosome with lysosomes. As mentioned above, our data suggest that CB1-KO prevents LC3 II accumulation, indicating restoration of the autophagy in mice fed a HFD. However, CB1-KO does not impact autophagic flux, suggesting that there is a compensation mechanism in KO mice; moreover, this experiment was not done in mice fed with a high-fat diet with ECS overactivation. An alternative explanation is that the CB1 regulates LC3 lipidation through competitive anandamide production. NAPE-PLD requires

calcium for the anandamide synthesis route, with phosphatidylethanolamine (PE) as a source [51]. PE is also a substrate for LC3 II production. It is known that CB1 regulates intracellular calcium flux [52]. Oláh et al. showed that the activation of the CB1 inhibits sarcoplasmic Ca^{2+} release and the sarcoplasmic reticulum Ca^{2+} ATPase during excitation–contraction coupling in a $G_{i/o}$ protein-mediated manner in adult skeletal muscle fibers. This could, in part, explain the reduction of LC3 II protein levels in mice injected with JD-5037; however, more research is necessary to confirm this hypothesis. Due to a possible effect on lysosomal function, we evaluated two lysosomal proteins, Lamp1 and Lamp2. Similarly, there was no difference between wild-type and CB1 KO, suggesting that the lysosome was unaffected. We also evaluated polyubiquitinated proteins at specific lysine residues (Lys48) because it labels proteins for proteasomal degradation. Interestingly, more polyubiquitinated proteins were found in mice treated with JD-5037. This result is consistent with the reduction of LC3 II protein, but the mechanism behind this is still elusive.

Contrary to our findings, Hiebel et al. [53] showed that siRNA knockdown of CB1 activity affects the autophagic flux independent of the canonical pathway. They performed an autophagic flux assay in human embryonic kidney cells, showing LC3 II accumulation, suggesting a possible role of the CB1 in autophagy regulation. Piyanova et al. [54] treated with Rapamycin (a known mTOR inhibitor that induces autophagy) and Baf1 (to inhibit autophagic flux) to hippocampal neurons from CB1-KO. LC3 II levels were higher in *Cnr1*^{-/-} neurons compared with *Cnr1*^{+/+}, indicating that the autophagic rate is higher in the absence of CB1. Moreover, Blázquez et al. [55] treated wild-type mice with a single *i.p.* injection of the Δ^9 -tetrahydrocannabinol (THC), which exerts its biological effects mainly by activating the CB1, and evaluated LC3 protein. LC3 II levels were increased, suggesting that THC impairs the autophagy and that this process occurs selectively in the striatum. Genetic background, mouse strain, diet composition, mice age, and cell line types could explain these discrepancies with our results. Additionally, TA in C57BL/6 mice is a fast-contracting muscle with a high percentage of type IIB fibers [56]. We explored mRNA levels of autophagy proteins but did not find alterations that could explain the reduction of LC3 protein levels. Additional autophagy or lysosomal genes and proteins should be assessed to elucidate these results.

Restoring autophagy levels in several diseases is key to recovering physiological processes. Autophagy is a potential target for developing pharmacological and non-pharmacological interventions to manage obesity. Therefore, it is relevant to search for new

pharmacological targets to counteract obesity-related disruptions in different physiological systems. Pharmacological blockers of the CB1, such as Rimonabant, were promising agents to reduce food intake and body weight and revert the metabolic alterations induced by obesity. However, its negative side effects related to severe complications of neuropsychiatric effects (i.e. anxiety, depression, and suicidal ideation) [57] led to its withdrawal from the market. The design of new CB1 peripheral blockers could remove these unwanted effects. JD-5037 exerts a positive impact on the control of body weight, metabolic outcome, and low brain penetration without adverse side effects [33]. However, in the current model, we observed that the inhibition of CB1 with JD-5037 produces a reduction of autophagic flux that needs further investigation.

It has been widely reported that obesity induces sarcopenia. In our results, CB1-KO prevents weight reduction in TA induced by a high-fat diet. Iannotti et al. (2014) showed in human and mouse myoblasts that the stimulation of CB1 with 2-AG or arachidonyl-2'-chloroethylamide prevents myotube formation and promotes myoblast proliferation. Interestingly, these effects are reverted with rimonabant [17]. Moreover, Iannotti et al. (2018) showed that treatment with rimonabant promotes human satellite cell differentiation in vitro and increases the number of myofibers [58]. However, Le Bacquer et al. (2022) cocultured C2C12 myotubes with dexamethasone and rimonabant for 24 h, and the atrophy was prevented in myotubes exposed to rimonabant, without affecting the atrogen-1/MAFbx ratio. The authors also found that rimonabant stimulates protein synthesis and CB1 agonists are unable to modulate protein synthesis, suggesting a CB1-independent mechanism [59]. In vitro and in vivo models, mouse strains, and rimonabant doses can explain these controversial results.

Conclusions

The present investigation provides evidence of altered autophagy in diet-induced obesity and increased “endocannabinoid tone.” Our results also indicate a regulatory role of the CB1 on fast muscle, such as the tibialis anterior in mice, reducing LC3 II accumulation induced by a HFD. In addition, acute pharmacological inhibition of the CB1 reduces LC3 II accumulation induced by chloroquine, suggesting a reduction of autophagic flux. In conclusion, CB1 regulates autophagy in the tibialis anterior muscle in mice. Although our study could not clarify why and how CB1 regulates autophagy, it opened a new area of research.

Methods

Animals and diet

All animal study protocols were reviewed and approved by the local Committee on Animal Health and Care of the University of Bordeaux and the Institute of Nutrition and Food Technology. For the first experiment, male C57BL/6 littermate mice were kept with food and tap water ad libitum, and a 12–12 h light–dark cycle. Mice were fed with a control diet (CD, $n=6$) containing 70% carbohydrates, 10% fat, and 20% protein in terms of kcal (Research Diet Inc. D12450J, New Brunswick, NJ, USA) and a high-fat diet (HFD, $n=6$) containing 60% fat (90% lard, 10% soybean oil), 20% carbohydrates and 20% protein in terms of kcal (D12492, Research Diets, New Brunswick, NJ, USA). Body weight and food intake were assessed weekly. At the end of the experiment, a glucose tolerance test (GTT) was performed. Finally, mice were euthanized, and the tibialis anterior (TA) muscle was removed for analysis.

For the second experiment, male C57BL/6 CB1^{+/+} (WT) and CB1^{-/-} (CB1-KO) littermate mice were maintained under standard conditions (food and tap water ad libitum; 12 h–12 h light–dark cycle). Mice were randomly assigned into 4 groups: WT CD (Wild-type control diet, $n=8$), WT HFD (Wild-type high-fat diet, $n=8$), CB1-KO CD (CB1 knockout control diet, $n=7$), and CB1-KO HFD (CB1 knockout high-fat diet, $n=6$). The mice were fed for 12 weeks with a chow diet containing 13.5% fat, 61.3% carbohydrates, and 25.2% protein in kcal (SAFE, A03 SP/17275) or a high-fat diet (D12492, Research Diets, New Brunswick, NJ, USA). Body weight and food intake were measured each week up to the end of the experiment. Body composition was also evaluated during the first and 12 week by nuclear echo magnetic resonance imaging whole-body composition analysis (EchoMRI 900; EchoMedical Systems, USA), as described previously [60]. Glycemia was measured in mice fasting for 6 h. Finally, the mice were sacrificed the next day after measuring the glycemia, and the TA was collected and frozen (-80°C). For the third experiment, mice were grouped in: WT PBS (Wild-type Phosphate-Buffered Saline; $n=5$), WT CQ (Wild-type chloroquine; $n=5$), CB1-KO PBS ($n=6$), and CB1-KO CQ ($n=7$). They fasted for 24 h and were subjected to an intraperitoneal injection of CQ (100 mg kg body weight) or PBS 4 h before sacrifice. Animals were sacrificed, and the TA muscle was quickly dissected and frozen for immunoblot analyses. For the fourth experiment, male C57BL/6 littermate mice were grouped in: CTRL (Control; $n=6$), CQ (chloroquine; $n=6$), JD (JD-5037; $n=6$), and JD-CQ ($n=6$). Mice were kept in fasting condition for 24 h. 4 h before sacrifice, mice were injected with 100 mg kg body

weight of chloroquine or PBS. After 2 h, an intraperitoneal injection of 3 mg kg⁻¹ body weight of JD-5037 or vehicle (1% DMSO, 1% Tween80, and PBS was applied. Finally, the animals were sacrificed, and the TA muscle was quickly dissected and frozen for immunoblot analyses.

Glucose tolerance test

Three days before sacrifice, a glucose tolerance test was performed in the morning. Mice fasted for 6 h in separated individual cages. Basal blood glucose was measured in samples collected from the tail with an Accu-Check Performa glucometer (Roche Diagnostic, Mannheim, Germany). Then, 1.5 mg kg⁻¹ body weight of glucose in PBS was injected intraperitoneally, and blood glucose was evaluated at 15, 30, 90, and 120 min time points. At the end of the assessment, mice were placed in their cages.

Endocannabinoid quantification

To determine endocannabinoids, we used the liquid chromatography-tandem mass spectrometric analysis method [61]. The blood samples of mice were collected and homogenized with chloroform/methanol (2:1, v/v) containing internal deuterated standards (Cayman Chemicals, Ann Arbor, MI, USA). Purified endocannabinoids were then evaluated by isotopic dilution, according to a calibration curve.

RNA extraction and PCR procedure

Total RNA was extracted from samples using a commercial kit (Fermentas, Villebon sur Yvette, France). Random hexamer primers and Oligo(dt)18 primers (Fermentas) were used for cDNA synthesis from 2 µg of total RNA with RevertAid Premium Reverse Transcriptase (Fermentas). Real-time PCR was performed using transcript-specific primers, cDNA (1 ng), and LightCycler 480 SYBR Green I Master (Roche) in a final volume of 10 µl. The 2-ΔΔCT method was used for relative quantification analysis, and PCR amplification of the housekeeping genes *Ywhaz*, *Gapdh*, and *Tubulin alpha* was used for controls. The primer's sequences are reported in Additional file 1: Table S1.

Western blot analyses

Total protein lysates were prepared using T-PER lysis buffer (78,510, ThermoScientific) with phosphatases/protease inhibitors. Lysates were centrifuged at 12,000 rpm for 10 min at 4 °C. Total protein concentrations were measured using the BCA assay kit (71,285-3, Novagen®, Merck, MA USA). Proteins were separated using 6–15% SDS-PAGE and transferred to PVDF membranes. The membranes were blocked with 5% low-fat milk (Svelty,

Nestlé) in T-TBS/0.1% (1 mM Tris) Tween-20 and incubated overnight at 4 °C with primary antibodies. The membranes were then extensively washed with TBS/0.1% Tween-20, and incubated with the secondary polyclonal anti-mouse (#402335, Calbiochem) or anti-rabbit (#401315, Calbiochem) antibodies. The protein bands in the blots were visualized using HRP secondary antibodies. Enhanced chemiluminescence ECL-plus reagent (DW1029, Biological Industries) and C-DiGit® Blot Scanner (LI-COR, USA) were used and bands were analyzed with the Image J version 1.51 software (National Institutes of Health, Bethesda, MD, USA). The primary antibodies used were CB1 (Cayman #10006590), LC3A/B (CST #4108), p62/Sqstm1 (NBP1-48320, Novus), GAPDH (CST #5174), phospho-p70S6K Thr389 (CST #9234), p70S6K Total (CST #2708), phospho-AMPKα Thr172 (CST #2535), AMPKα Total (CST #5831), phospho-Akt Ser473 (CST #9271), Akt Total (CST #9272), phospho-mTOR Ser2448 (CST #2971), mTOR total (CST #2972), Lamp1 (CST #3243), Lamp2 (CST #49,067), and K48-linkage Specific Polyubiquitin (CST # 4289). GAPDH or total protein content were used as loading controls.

Statistical analysis

All values are presented as mean ± standard error of the mean (SEM). Statistical analyses were performed using Student's t-test, repeated measure analysis of variance (ANOVA), and two-way ANOVA for non-repeated measures. Diet—genotype, genotype—chloroquine, and JD-5037—chloroquine were used as the main effects for the variables. Bonferroni's post hoc test was applied where appropriate, and statistical significances were set at $p < 0.05$. All statistical analyses were performed using the GraphPad Prism software (version 8.0, San Diego, CA, USA).

Abbreviations

2-AG	2-Arachidonoylglycerol
AEA	Arachidonylethanolamide or anandamide
CB1	Type 1 cannabinoid receptor
CD	Control diet
CQ	Chloroquine
Dagla	Diacylglycerol lipase alpha
Daglb	Diacylglycerol lipase beta
ECS	Endocannabinoid system
FAAH	Fatty acid amide hydrolase
GTT	Glucose tolerance test
HFD	High-fat diet
KO	Knockout
Lamp1	Lysosomal-associated protein 1
Lamp2	Lysosomal-associated protein 2
LC3-I	Microtubule-associated protein 1 light chain 3
LC3-II	Phosphatidylethanolamine conjugated form of microtubule associated protein 1 light chain 3
MAGL	Monoacylglycerol lipase
Napepld	N-acyl phosphatidylethanolamine phospholipase D

OEA	Oleoylethanolamine
PEA	N-palmitoyl-ethanolamine
PE	Phosphatidylethanolamine
TA	Tibialis anterior
WT	Wild type

Supplementary Information

The online version contains supplementary material available at <https://doi.org/10.1186/s40659-023-00426-5>.

Additional file 1: Representative western blot image.

Acknowledgements

We thank Dr. Giovanni Marsicano (INSERM U1215, Bordeaux) for providing the CB1-KO mice, and Samantha Clark (INSERM U1215, Bordeaux) for her technical help. We thank the animal housing, genotyping, transcriptomic and analytical chemistry facilities of INSERM U1215 Neurocentre Magendie, and also for animal caring, genotyping, qPCR studies, and quantification of endocannabinoids.

Author contributions

CS contributed to the conceptualization, methodology, investigation, formal analysis, writing-original draft preparation, editing, and visualization. JMR and MMA contributed to the investigation, formal analysis, and review. CDB, FPFIM, TLL and PZ contributed to the formal analysis and investigation. DC and EM contributed to the methodology, formal analysis, and editing of the manuscript. MLI and RT contributed to the conceptualization, methodology, supervision, and visualization, and provided resources and funding acquisition. All authors read and approved the final manuscript.

Funding

C.S. was supported by CONICYT Ph.D. Scholarship N° 21180609, and "Proyecto de Consolidación de la Internacionalización de la Investigación y Postgrado de la Universidad de Chile, UCH-1566" (C.S.). R.T. was supported by Agencia Nacional de Investigación y Desarrollo (ANID), Chile: FONDAPE 15130011 and FONDECYT 1191078. D. C. was supported by INSERM, Aquitaine Region and French National Research Agency (ANR, ANR-17-CE14-0007 BABrain, ANR-18-CE14-0029 MitObesity, Labex BRAIN ANR-10-LABX-43, ANR-10-EQX-008-1 OPTOPATH). The platform facilities of INSERM U1215 Neurocentre Magendie used for the studies are supported by INSERM, LabEX BRAIN ANR-10-LABX-43 and the University of Bordeaux's IdEx "Investments for the Future" program/ GPR BRAIN_2030. Institutional Review Board Statement: The animal study protocol was approved by the Instituto de Nutrición y Tecnología de los Alimentos (Project Identification Code N° 17,073-INT-UCH).

Availability of data and materials

The data that support the findings of this study are available from the corresponding authors (C.S. and R.T.) upon reasonable request.

Declarations

Ethics approval and consent to participate

Not applicable.

Consent for publication

All the authors have read and approved the paper for publication.

Competing interests

The authors declare that they have no competing interests.

Received: 26 August 2022 Accepted: 15 March 2023

Published online: 25 March 2023

References

- Gregg EW, Shaw JE. Global health effects of overweight and obesity. *N Engl J Med*. 2017;377:80–1.
- Flegal KM, Kruszon-Moran D, Carroll MD, Fryar CD, Ogden CL. Trends in obesity among adults in the United States, 2005 to 2014. *JAMA*. 2016;315:2284–91.
- Ogden CL, Carroll MD, Lawman HG, Fryar CD, Kruszon-Moran D, Kit BK, et al. Trends in obesity prevalence among children and adolescents in the United States, 1988–1994 Through 2013–2014. *JAMA*. 2016;315:2292–9.
- Hafekost K, Lawrence D, Mitrou F, O'Sullivan TA, Zubrick SR. Tackling overweight and obesity: does the public health message match the science? *BMC Med*. 2013;11:41.
- Galluzzi L, Pietrocola F, Levine B, Kroemer G. Metabolic control of autophagy. *Cell*. 2014;159:1263–76.
- Che Y, Wang Z-P, Yuan Y, Zhang N, Jin Y-G, Wan C-X, et al. Role of autophagy in a model of obesity: a long-term high fat diet induces cardiac dysfunction. *Mol Med Rep*. 2018;18:3251–61.
- Masiero E, Agatea L, Mammucari C, Blaauw B, Loro E, Komatsu M, et al. Autophagy is required to maintain muscle mass. *Cell Metab*. 2009;10:507–15.
- Jiang P, Mizushima N. Autophagy and human diseases. *Cell Res Nature Publ Group*. 2014;24:69–79.
- Neel BA, Lin Y, Pessin JE. Skeletal muscle autophagy: a new metabolic regulator. *Trends Endocrinol Metab*. 2013. <https://www.ncbi.nlm.nih.gov/pmc/articles/PMC3849822/>
- Sebastián D, Zorzano A. Self-eating for muscle fitness: autophagy in the control of energy metabolism. *Dev Cell*. 2020;54:268–81.
- Fan J, Kou X, Jia S, Yang X, Yang Y, Chen N. Autophagy as a potential target for sarcopenia. *J Cell Physiol*. 2016;231:1450–9.
- Pagotto U, Marsicano G, Cota D, Lutz B, Pasquali R. The emerging role of the endocannabinoid system in endocrine regulation and energy balance. *Endocr Rev*. 2006;27:73–100.
- Simon V, Cota D. Mechanisms in endocrinology: endocannabinoids and metabolism: past, present and future. *Eur J Endocrinol*. 2017;176:R309–24.
- Matias I, Gatta-Cherifi B, Cota D. Obesity and the endocannabinoid system: circulating endocannabinoids and obesity. *Curr Obes Rep*. 2012;1:229–35.
- Osei-Hyiaman D, DePetrillo M, Pacher P, Liu J, Radaeva S, Bátkai S, et al. Endocannabinoid activation at hepatic CB1 receptors stimulates fatty acid synthesis and contributes to diet-induced obesity. *J Clin Invest*. 2005;115:1298–305.
- Matias I, Gonthier M-P, Orlando P, Martiadis V, De Petrocellis L, Cervino C, et al. Regulation, function, and dysregulation of endocannabinoids in models of adipose and beta-pancreatic cells and in obesity and hyperglycemia. *J Clin Endocrinol Metab*. 2006;91:3171–80.
- Iannotti FA, Silvestri C, Mazzarella E, Martella A, Calvigioni D, Piscitelli F, et al. The endocannabinoid 2-AG controls skeletal muscle cell differentiation via CB1 receptor-dependent inhibition of Kv7 channels. *Proc Natl Acad Sci U S A*. 2014;111:E2472–81.
- Esposito I, Proto MC, Gazerro P, Laezza C, Miele C, Alberobello AT, et al. The cannabinoid CB1 receptor antagonist rimonabant stimulates 2-deoxyglucose uptake in skeletal muscle cells by regulating the expression of phosphatidylinositol-3-kinase. *Mol Pharmacol*. 2008;74:1678–86.
- Jbilo O, Ravinet-Trillou C, Arnone M, Buisson I, Bribes E, Péleraux A, et al. The CB1 receptor antagonist rimonabant reverses the diet-induced obesity phenotype through the regulation of lipolysis and energy balance the FASEB journal. *Fed Am Soc Exp Biol*. 2005. <https://doi.org/10.1096/fj.04-3177fje>.
- Nogueiras R, Veyrat-Durebex C, Suchanek PM, Klein M, Tschöp J, Caldwell C, et al. Peripheral, but not central, CB1 antagonism provides food intake-independent metabolic benefits in diet-induced obese rats. *Diabetes Am Diabetes Assoc*. 2008;57:2977–91.
- Osei-Hyiaman D, Liu J, Zhou L, Godlewski G, Harvey-White J, Jeong W, et al. Hepatic CB1 receptor is required for development of diet-induced steatosis, dyslipidemia, and insulin and leptin resistance in mice. *J Clin Invest*. 2008;118:3160–9.

22. Scerif M, Füzesi T, Thomas JD, Kola B, Grossman AB, Fekete C, et al. CB1 receptor mediates the effects of glucocorticoids on AMPK activity in the hypothalamus. *J Endocrinol BioSci*. 2013;219:79–88.
23. Bermudez-Silva FJ, Romero-Zerbo SY, Haissaguerre M, Ruz-Maldonado I, Lhamyani S, El Bekay R, et al. The cannabinoid CB1 receptor and mTORC1 signalling pathways interact to modulate glucose homeostasis in mice. *Dis Model Mech*. 2016;9:51–61.
24. Kataoka K, Bilkei-Gorzo A, Nozaki C, Togo A, Nakamura K, Ohta K, et al. Age-dependent alteration in mitochondrial dynamics and autophagy in hippocampal neuron of cannabinoid CB1 receptor-deficient mice. *Brain Res Bull*. 2020. <https://doi.org/10.1016/j.brainresbull.2020.03.014>.
25. Lin B, Gao Y, Li Z, Zhang Z, Lin X, Gao J. Cannabidiol alleviates hemorhagic shock-induced neural apoptosis in rats by inducing autophagy through activation of the PI3K/AKT pathway. *Fundam Clin Pharmacol*. 2020;34:640–9.
26. Cota D. CB1 receptors: emerging evidence for central and peripheral mechanisms that regulate energy balance, metabolism, and cardiovascular health. *Diabetes Metab Res Rev*. 2007;23:507–17.
27. Heyman E, Gamelin F-X, Aucouturier J, Di Marzo V. The role of the endocannabinoid system in skeletal muscle and metabolic adaptations to exercise: potential implications for the treatment of obesity. *Obes Rev*. 2012;13:1110–24.
28. Sam S, Mazzone T. Adipose tissue changes in obesity and the impact on metabolic function. *Transl Res*. 2014;164:284–92.
29. Lin X, Li H. Obesity: epidemiology, pathophysiology, and therapeutics. *Front Endocrinol*. 2021;12: 706978.
30. Mofarrah M, Guo Y, Haspel JA, Choi AMK, Davis EC, Gouspillou G, et al. Autophagic flux and oxidative capacity of skeletal muscles during acute starvation. *Autophagy*. 2013;9:1604–20.
31. Wu JJ, Quijano C, Chen E, Liu H, Cao L, Fergusson MM, et al. Mitochondrial dysfunction and oxidative stress mediate the physiological impairment induced by the disruption of autophagy. *Aging*. 2009;1:425–37.
32. Ravinet Trillou C, Delgorgue C, Menet C, Arnone M, Soubrié P. CB1 cannabinoid receptor knockout in mice leads to leanness, resistance to diet-induced obesity and enhanced leptin sensitivity. *Int J Obes Relat Metab Disord*. 2004;28:640–8.
33. Quarta C, Cota D. Anti-obesity therapy with peripheral CB1 blockers: from promise to safe (?) practice. *Int J Obes*. 2020. <https://doi.org/10.1038/s41366-020-0577-8>.
34. You T, Disanzo BL, Wang X, Yang R, Gong D. Adipose tissue endocannabinoid system gene expression: depot differences and effects of diet and exercise. *Lipids Health Dis*. 2011;10:194.
35. Lopez Trinidad LM, Martínez R, Kapravelou G, Galisteo M, Aranda P, Porres JM, et al. Caloric restriction, physical exercise, and CB1 receptor blockade as an efficient combined strategy for bodyweight control and cardio-metabolic status improvement in male rats. *Sci Rep*. 2021;11:4286.
36. Massa F, Mancini G, Schmidt H, Steindel F, Mackie K, Angioni C, et al. Alterations in the hippocampal endocannabinoid system in diet-induced obese mice. *J Neurosci Soc Neurosci*. 2010;30:6273–81.
37. Lillo A, Lillo J, Raich I, Miralpeix C, Dosrius F, Franco R, et al. Ghrelin and cannabinoid functional interactions mediated by ghrelin/CB1 receptor heteromers that are upregulated in the striatum from offspring of mice under a high-fat diet. *Front Cell Neurosci*. 2021;15: 786597.
38. Liu YL, Connoley IP, Wilson CA, Stock MJ. Effects of the cannabinoid CB1 receptor antagonist SR141716 on oxygen consumption and soleus muscle glucose uptake in Lep(ob)/Lep(ob) mice. *Int J Obes (Lond)*. 2005;29:183–7.
39. Dainese E, Oddi S, Simonetti M, Sabatucci A, Angelucci CB, Ballone A, et al. The endocannabinoid hydrolase FAAH is an allosteric enzyme. *Sci Rep*. 2020;10:2292.
40. Sipe JC, Waalen J, Gerber A, Beutler E. Overweight and obesity associated with a missense polymorphism in fatty acid amide hydrolase (FAAH). *Int J Obes (Lond)*. 2005;29:755–9.
41. Touriño C, Oveisi F, Lockney J, Piomelli D, Maldonado R. FAAH deficiency promotes energy storage and enhances the motivation for food. *Int J Obes (Lond)*. 2010;34:557–68.
42. Meng Q, Cai D. Defective hypothalamic autophagy directs the central pathogenesis of obesity via the IkkappaB kinase beta (IKKbeta)/NF-kappaB pathway. *J Biol Chem*. 2011;286:32324–32.
43. Yang L, Li P, Fu S, Calay ES, Hotamisligil GS. Defective hepatic autophagy in obesity promotes ER stress and causes insulin resistance. *Cell Metab*. 2010;11:467–78.
44. de Sousa LGO, Marshall AG, Norman JE, Fuqua JD, Lira VA, Rutledge JC, et al. The effects of diet composition and chronic obesity on muscle growth and function. *Journal of applied physiology*. *Am Physiol Soc*. 2021;130:124–38.
45. Barth S, Glick D, Macleod KF. Autophagy: assays and artifacts. *J Pathol*. 2010;221:117–24.
46. Fan Z, Xiao Q. Impaired autophagic flux contributes to muscle atrophy in obesity by affecting muscle degradation and regeneration. *Biochem Biophys Res Commun*. 2020;525:462–8.
47. Li J, Kanasaki M, Xu L, Kitada M, Nagao K, Adachi Y, et al. A ketogenic amino acid rich diet benefits mitochondrial homeostasis by altering the AKT/4EBP1 and autophagy signaling pathways in the gastrocnemius and soleus. *Biochim Biophys Acta*. 2018;1862:1547–55.
48. Dupont N, Codogno P. Non-canonical autophagy: facts and prospects. *Curr Pathobiol Rep*. 2013;1:263–71.
49. Yoshii SR, Mizushima N. Monitoring and measuring autophagy. *Int J Mol Sci*. 2017;18:1865.
50. Klionsky DJ, Abdel-Aziz AK, Abdelfatah S, Abdellatif M, Abdoli A, Abel S, et al. Guidelines for the use and interpretation of assays for monitoring autophagy. *Autophagy*. 2021;17:1–382.
51. Ogura Y, Parsons WH, Kamat SS, Cravatt BF. A calcium-dependent acyltransferase that produces N-acyl phosphatidylethanolamines. *Nat Chem Biol*. 2016;12:669–71.
52. Oláh T, Bodnár D, Tóth A, Vincze J, Fodor J, Reischl B, et al. Cannabinoid signalling inhibits sarcoplasmic Ca²⁺ release and regulates excitation-contraction coupling in mammalian skeletal muscle. *J Physiol*. 2016;594:7381–98.
53. Hiebel C, Kromm T, Stark M, Behl C. Cannabinoid receptor 1 modulates the autophagic flux independent of mTOR- and BECLIN1-complex. *J Neurochem*. 2014;131:484–97.
54. Piyanova A, Albayram O, Rossi CA, Farwanah H, Michel K, Nicotera P, et al. Loss of CB1 receptors leads to decreased cathepsin D levels and accelerated lipofuscin accumulation in the hippocampus. *Mech Ageing Dev*. 2013;134:391–9.
55. Blázquez C, Ruiz-Calvo A, Bajo-Grañeras R, Baufretton JM, Resel E, Varilh M, et al. Inhibition of striatonigral autophagy as a link between cannabinoid intoxication and impairment of motor coordination. *Elife*. 2020. <https://doi.org/10.7554/eLife.56811>.
56. Giacomello E, Crea E, Torelli L, Bergamo A, Reggiani C, Sava G, et al. Age dependent modification of the metabolic profile of the tibialis anterior muscle fibers in C57BL/6J mice. *Int J Mol Sci*. 2020;21:E3923.
57. Christensen R, Kristensen PK, Bartels EM, Bliddal H, Astrup A. Efficacy and safety of the weight-loss drug rimonabant: a meta-analysis of randomised trials. *Lancet*. 2007;370:1706–13.
58. Iannotti FA, Pagano E, Guardiola O, Adinolfi S, Saccone V, Consalvi S, et al. Genetic and pharmacological regulation of the endocannabinoid CB1 receptor in duchenne muscular dystrophy. *Nat Commun*. 2018;9:3950.
59. Le Bacquer O, Lanchais K, Combe K, Van Den Berghe L, Walrand S. Acute rimonabant treatment promotes protein synthesis in C2C12 myotubes through a CB1-independent mechanism. *J Cell Physiol*. 2021;236:2669–83.
60. Castellanos-Jankiewicz A, Guzmán-Quevedo O, Fénelon VS, Zizzari P, Quarta C, Bellocchio L, et al. Hypothalamic bile acid-TGR5 signaling protects from obesity. *Cell Metab*. 2021;33:1483-1492.e10.
61. Gatta-Cherifi B, Matias I, Vallée M, Tabarin A, Marsicano G, Piazza PV, et al. Simultaneous postprandial deregulation of the orexigenic endocannabinoid anandamide and the anorexigenic peptide YY in obesity. *Int J Obes*. 2012;36:880–5.

Publisher's Note

Springer Nature remains neutral with regard to jurisdictional claims in published maps and institutional affiliations.